Published in final edited form as:

Oncogene. 2015 August 27; 34(35): 4624–4634. doi:10.1038/onc.2014.392.

Mortalin (GRP75/HSPA9) upregulation promotes survival and proliferation of medullary thyroid carcinoma cells

Dmytro Starenki[1], **Seung-Keun Hong**[1], **Ricardo V. Lloyd**[2], and **Jong-In Park**[1]

[1]Department of Biochemistry, Medical College of Wisconsin, Milwaukee, WI 53226, USA

[2]Department of Pathology and Laboratory Medicine, University of Wisconsin, Madison, WI 53792, USA

Abstract

Medullary thyroid carcinoma (MTC) is a neuroendocrine tumor mainly caused by mutations in the *RET* proto-oncogene. For therapy of advanced MTC, the Food and Drug Administration recently approved vandetanib and cabozantinib, the tyrosine kinase inhibitors targeting RET, vascular endothelial growth factor receptor, epidermal growth factor receptor, and/or c-MET. Nevertheless, not all patients respond to these drugs, demanding additional therapeutic strategies. We found that mortalin (HSPA9/GRP75), a member of HSP70 family, is upregulated in human MTC tissues and that its depletion robustly induces cell death and growth arrest in MTC cell lines in culture and in mouse xenografts. These effects were accompanied by substantial downregulation of *RET*, induction of the tumor suppressor TP53, and altered expression of cell cycle regulatory machinery and apoptosis markers including E2F-1, $p21^{CIP1}$, $p27^{KIP1}$, and Bcl-2 family proteins. Our investigation of the molecular mechanisms underlying these effects revealed that mortalin depletion induces transient MEK/ERK activation and altered mitochondrial bioenergetics in MTC cells, as indicated by depolarized mitochondrial membrane, decreased oxygen consumption and extracellular acidification, and increased oxidative stress. Intriguingly, mortalin depletion induced growth arrest partly via the MEK/ERK pathway whereas it induced cell death by causing mitochondrial dysfunction in a Bcl-2 dependent manner. However, TP53 was not necessary for these effects except for $p21^{CIP1}$ induction. Moreover, mortalin depletion downregulated RET expression independently of MEK/ERK and TP53. These data demonstrate that mortalin is a key regulator of multiple signaling and metabolic pathways pivotal to MTC cell survival and proliferation, proposing mortalin as a novel therapeutic target for MTC.

Keywords

Medullary thyroid carcinoma; mortalin/GRP75/HSPA9; mitochondria; RET; ERK1/2

Corresponding author: Jong-In Park Department of Biochemistry, Medical College of Wisconsin, 8701 Watertown Plank Road, Milwaukee, WI 53226, USA Phone: +1 (414) 955-4098 Fax : +1 (414) 955-6510 jipark@mcw.edu (J.-I.P.).

Conflict of interest

The authors have no conflict of interest to declare.

Introduction

Medullary thyroid carcinoma (MTC) is a neoplasm of the endocrine system, originating from parafollicular C-cells of the thyroid gland which produce the hormone calcitonin [1]. MTC occurs sporadically or in hereditary forms, i.e., familial MTC and multiple endocrine neoplasia (MEN) type 2 syndrome. MTC is relatively rare, comprising about 5% of all thyroid cancers, and progresses slowly. Although extensive surgical resection of thyroid and lymph nodes is mostly curative for primary MTC, it is not effective for metastatic or recurrent MTC. Because MTC rarely responds to classic chemo- or radiation-therapies, more advanced therapeutic modalities are necessary. MTC is mainly caused by altered activity of the receptor tyrosine kinase, rearranged during transfection (RET), while other oncogenic alterations including H- and K-Ras mutations are also detected in MTC at lower frequencies [2-4]. Accordingly, current therapeutic strategies for MTC are focused on RET inhibition, and for surgically inoperable progressive MTC treatment, the Food and Drug Administration recently approved vandetanib (trade name Caprelsa, AstraZeneca) and cabozantinib (Cometriq, Exelixis), the multi-kinase inhibitors targeting RET and a few other receptor tyrosine kinases [5, 6]. Nevertheless, these drugs are not always effective, demanding additional therapeutic strategies for treatment of MTC [5-7].

Mortalin (HSPA9/GRP75/PBP74), a member of the heat shock protein (HSP) 70 family [8], is often overexpressed in different tumor types, including colon, liver, brain, breast, and skin cancers [9-12]. Although mortalin was originally identified as a mitochondrial molecular chaperone [13], it is often detected in different subcellular compartments of cancer cells, suggesting its functional alteration in cancer [10, 11, 14]. Indeed, mortalin has been characterized as an important regulator of tumor cell growth and survival. For example, mortalin can mediate cytoplasmic sequestration of TP53 for negatively regulation of the tumor suppressor in different tumor types [15-19]. Mortalin could also affect Ras activity via its interaction with mevalonate pyrophosphate decarboxylase, which regulates Ras modification [20]. Moreover, we recently reported that mortalin can regulate the Raf/MEK/ERK pathway to promote proliferation and that mortalin upregulation may be important for B-Raf^{V600E} cancer cells to bypass tumor suppressive responses triggered upon aberrant MEK/ERK activation [12]. Mortalin may facilitate tumor cell growth and survival via additional functions.

In this study, we demonstrate that mortalin is upregulated in human MTC tissues and that it has a pivotal role for MTC cell survival and proliferation, which are mediated via the MEK/ERK pathway and mitochondrial bioenergetics in a distinct manner. Our data suggest that mortalin is a key regulator of cell signaling and metabolism in MTC cells and, thus, a novel therapeutic target for MTC treatment.

Results

Mortalin levels are upregulated in MTC

To examine mortalin levels in MTC, we conducted immunohistochemical analysis of 38 cases of MTC patient tissues in comparison with 46 normal thyroid tissues. Using a mortalin-specific antibody previously validated for IHC [12], we found that mortalin protein

levels were significantly upregulated in the MTC tissues (Fig. 1A and 1B; H&E staining shown in Supplemental Fig. S1). Consistent with this, our Western blot analysis revealed that mortalin levels are relatively high in the human MTC cell lines, TT and MZ-CRC-1, when compared with the primary normal human fibroblasts, and a positive control, MCF7 breast cancer cell line (Fig. 1C). MCF7 cells were previously shown to express mortalin relatively highly among different cancer cell lines derived from tumors of breast, prostate, colon, lung, and brain [11]. TT and MZ-CRC-1, expressing RET^{C634W} and RET^{M918T} respectively, are the most thoroughly characterized MTC lines and have been extensively used to study molecular mechanisms underlying the pathogenesis of MTC. RET^{C634W} and RET^{M918T} are most frequently detected oncogenic alterations in MTC, representing MEN type 2A and 2B respectively [21]. We therefore investigated the role of mortalin in MTC using these cell line models.

Mortalin depletion induces cell cycle arrest in G0/G1 phase, apoptotic cell death, and RET downregulation in MTC cells

Using lentiviral doxycycline-inducible small hairpin RNA (shRNA) expression system (shMortmir) and transient shRNA expression system (shMort) that target different mRNA regions, mortalin was substantially depleted in TT and MZ-CRC-1 cells (Fig. 2A and 2B; Fig. 6B shows shMortmir effects in MZ-CRC-1). In these cell lines, mortalin depletion consistently induced substantial downregulation of the S-phase transcription factor, E2F-1; expression of the cyclin-dependent kinase inhibitor, $p27^{KIP1}$; cleavage of the caspase-dependent apoptosis marker, poly (ADP-ribose) polymerase (PARP); and RET downregulation (Fig. 2A and 2B). Importantly, as demonstrated in TT cells, expression of an exogenous mortalin gene engineered to avoid shMortmir (HA-Mort*) significantly abolished shMortmir effects, indicating that these are specific effects of mortalin depletion (Fig. 2C).

In agreement with these effects, mortalin knockdown strongly suppressed cell viability of TT and MZ-CRC-1 in culture (Fig. 2D and 2E), which was significantly attenuated by HAMort* expression, as determined in TT cells (Fig. 2F). Cell cycle analysis and annexin V staining revealed that mortalin depletion suppressed MTC cell growth partly via G0/G1-phase cell cycle arrest (Fig. 2G and 2H) and apoptosis (Fig. 2I). We also found that mortalin depletion induced RET downregulation at mRNA level. As determined by RT-PCR, mortalin depletion significantly decreased the levels of *RET* splicing variants, RET51/variant 2 and RET9/variant 4 (Fig. 2J). In contrast, mortalin depletion did not significantly affect mRNA levels of calcitonin gene splicing variants, *CT* and *CGRP* (Fig. 2J), highlighting its specific effect on RET. These data suggest that mortalin is important for MTC cell proliferation and survival.

TP53 is not necessary for mortalin depletion to induce growth inhibition in MTC cells

It was previously reported that mortalin can sequester TP53 in the cytosol, subsequently inducing TP53 degradation and decreasing cellular tumor suppressive capacity [15-17]. Because TT cells express wild type TP53 (Cancer Genome Project at Sanger Institute, http://www.sanger.ac.uk/), we determined whether TP53 was required for mortalin depletion to suppress TT cell growth/survival. In TT cells, mortalin depletion mildly increased TP53

levels, which was accompanied by significant upregulation of $p21^{CIP1}$, a cyclin-dependent kinase inhibitor transcriptionally regulated by TP53 (Fig. 3A). When TP53 was depleted under this condition by RNA interference, shMortmir-induced $p21^{CIP1}$ upregulation was substantially inhibited (Fig. 3A). Nevertheless, TP53 knockdown did not affect shMortmir-induced PARP cleavage, E2F1 downregulation, $p27^{KIP1}$ upregulation, RET downregulation (Fig. 3A), and growth arrest (Fig. 3B), suggesting that TP53 is not necessary for mortalin depletion to suppress MTC cell proliferation and survival.

The MEK/ERK pathway mediates mortalin depletion-induced growth arrest but not cell death

The MEK/ERK pathway can mediate growth arrest signaling in MTC cells via various mechanisms [22-26]. Because we recently discovered that mortalin can modulate MEK/ERK activity [12], we questioned whether mortalin depletion suppressed MTC cell growth/survival by altering MEK/ERK signaling. Indeed, as determined by ERK1/2 phosphorylation on the activation loop (Thr202/Tyr204 for ERK1 and Thr183/Tyr185 for ERK2), mortalin depletion increased MEK/ERK activity in TT and MZ-CRC-1 cells (Fig. 2A and 2B). In a subsequent time-course study using TT cells stably expressing shMortmir, we found that mortalin depletion induced transient MEK/ERK activation prior to the aforementioned growth inhibitory effects (Supplemental Fig. S2B).

We next determined whether the MEK1/2 inhibitor, AZD6244, or MEK1/2 knockdown could block shMortmir effects in TT cells. Short term AZD6244 treatment or knockdown of both MEK1 and MEK2, albeit not singly knockdown, significantly reduced ERK1/2 phosphorylation (Fig. 3C and 3D). Under these conditions, shMortmir-induced E2F-1 downregulation and $p27^{KIP1}$ expression was mildly but consistently attenuated (Fig.3C and 3D). Consistent with these effects, AZD6244 could partially rescue TT cells from shMortmir-induced growth suppression (Fig. 3E) and cell cycle arrest (Fig. 3F). However, interestingly, neither AZD6244 nor MEK1/2 knockdown inhibited shMortmir-induced PARP cleavage and RET downregulation (Fig. 3C and 3D). These data indicate that the MEK/ERK pathway is specifically involved in mortalin depletion-induced growth arrest, but not cell death or RET downregulation, in MTC cells.

Mortalin depletion disrupts mitochondrial activity in MTC cells

Mitochondrial damages often induce cell death signals [27]. Because neither TP53 nor the MEK/ERK pathway was necessary for mortalin depletion-induced cell death, we questioned whether mortalin depletion induced cell death by altering mitochondrial integrity in MTC cells. To test this possibility, we first determined mortalin localization in TT and MZ-CRC-1 cells by immunofluorescence. Confocal microscopy of these cells stained for mortalin and the mitochondrial marker, cytochrome *c* oxidase (COX IV), revealed highly overlapping signals of these proteins (overlap coefficient = 0.9), suggesting that mortalin is mainly localized in mitochondria in MTC cells (Fig. 4A).

Given this observation, we determined the effects of mortalin knockdown on mitochondrial activity by examining mitochondrial membrane potential ($\Delta\psi_m$) using tetramethyl-rhodamine ethyl ester perchlorate (TMRE). Upon mortalin depletion, TT cells exhibited

significantly decreased TMRE staining (Fig. 4B, upper panel), which was substantially abolished by HAMort* overexpression (Fig. 4B, lower panel). In contrast, AZD6244 did not affect the degree of TMRE staining in the control or mortalin-depleted cells. These data suggest that mortalin depletion induces loss of mitochondrial membrane potential in MTC cells, and that MEK/ERK activity is not necessary for that effect.

We next determined whether mortalin depletion could also affect the oxygen consumption rate (OCR). In this analysis, we used different inhibitors of the electron transport chain to determine the multiple parameters of mitochondrial function previously described [28]. Briefly, the ATPase inhibitor oligomycin allows measurement of basal OCR; the uncoupler FCCP yields maximal OCR; and the complex III inhibitor antimycin A blocks all mitochondrial oxygen consumption, allowing measurement of mitochondrial components of respiration. We found that mortalin depletion substantially reduced basal as well as maximal OCR in TT cells, which suggests decreased ATP production and mitochondrial respiratory capacity (Fig. 4D). Moreover, our time-course analysis revealed that mortalin depletion also significantly decreased the extracellular acidification rate (ECAR) along with decreased basal OCR (Fig. 4E), suggesting decreased glycolytic rates. These data suggest that mortalin is pivotal to mitochondrial activity and bioenergetics in MTC cells.

Mortalin depletion induces cell death via oxidative stress and downregulation of the bcl-2 family proteins in MTC cells

Because mitochondrial damages often initiate cell death via oxidative stress [29], we determined whether mortalin depletion induced oxidative stress in MTC cells using the redox-sensitive fluorescent dye, 5-(and-6)-carboxy-2',7'-dichlorodihydrofluorescein diacetate (carboxy-H_2DCFDA). We detected significantly increased carboxy-H_2DCFDA fluorescence in mortalin-depleted TT cells (Fig. 5A). This effect was accompanied by substantially increased lamin A cleavage but significant decreases in anti-apoptotic proteins, Bcl-2, Bcl-xL, and Mcl-1 (Fig. 5B). Along with these effects, COX IV levels were also significantly decreased upon mortalin depletion, suggesting an onset of mitochondrial stress (Fig. 5B). HA-Mort* expression abolished all these effects, confirming that they are mortalin depletion-specific effects (Fig. 5B).

Because the bcl-2 family proteins respond to oxidative stress [29], we suspected that oxidative stress and subsequent decreases in the anti-apoptotic proteins may account for MTC cell death induced by mortalin depletion. This possibility was tested by determining whether the reactive oxygen species scavenger N-acetyl cysteine (NAC), Bcl-2 overexpression, or the broad spectrum caspase inhibitor Z-VAD(OMe)-FMK could abrogate shMortmir effects in TT cells. In a time-course analysis, we observed that NAC mildly delayed shMortmir-induced cleavage of PARP and lamin A (Fig. 5C, middle panel) whereas Bcl-2 overexpression substantially inhibited cleavage of these caspase substrates (Fig. 5C, right panel). Z-VAD(OMe)-FMK also effectively blocked shMortmir-induced cleavage of PARP and lamin A (Fig. 5D). These data strongly suggest that mortalin depletion induces caspase-dependent apoptotic cell death via oxidative stress and by regulating the bcl-2 family proteins in MTC cells.

Bcl-2 overexpression does not inhibit growth arrest induced by mortalin depletion

In contrast to its ability to inhibit shMortmir-induced PARP and lamin A cleavage, Bcl-2 overexpression did not inhibit shMortmir-induced E2F-1 downregulation and $p27^{KIP1}$ induction in TT cells (Fig. 5C, right panel). Bcl-2 overexpression did not also affect shMortmir-induced ERK1/2 activation (Fig. 5C), while AZD6244 inhibited shMortmir-induced E2F-1 downregulation and $p27^{KIP1}$ induction irrespective to bcl-2 overexpression (Fig. 5E). These data suggest that, contrary to its significance for cell survival, Bcl-2 is not critical for growth arrest induced by mortalin depletion. Intriguingly, neither Bcl-2 overexpression nor Z-VAD(OMe)-FMK inhibited shMortmir-induced RET downregulation, although it was mildly inhibited by NAC treatment (Fig. 5C and 5D). Together, these data suggest that mortalin depletion triggers growth arrest, cell death, and RET downregulation via distinct mechanisms, wherein the MEK/ERK pathway mediates growth arrest; the mitochondrial apoptotic pathway mediates cell death; and RET downregulation is mediated independently of MEK/ERK, Bcl-2, and TP53 (Fig. 5F).

Mortalin depletion effectively suppresses MTC xenografts in mice

To further evaluate mortalin as a potential therapeutic target, we examined the effects of mortalin depletion on MTC mouse xenografts derived from TT and MZ-CRC-1 cells stably harboring shMortmir. Administration of doxycycline significantly suppressed tumor growth, inducing tumor shrinkage almost to the levels of complete regression in both TT and MZ-CRC-1 xenografts harboring shMortmir (Fig. 6A). However, doxycycline did not induce any tumor suppressive effects in the control tumors. When doxycycline administration was curtailed at day 20 from its initiation (thus mortalin depletion was no longer induced), tumors began to relapse in all cases in the test groups and resumed growth at similar rates as detected in the control groups (Fig. 6A). During this experiment, the host animals did not exhibit any significant side effects other than the tumor-associated responses.

We also harvested MTC tumors during the doxycycline treatment (day 10) and examined tumor homogenates by Western blotting for those aforementioned markers of growth arrest and cell death (Fig. 6B). In both TT and MZ-CRC-1 xenografts, mortalin depletion was accompanied by significant decreases in RET and E2F-1, and increases in $p27^{KIP1}$ and ERK1/2 phosphorylation (Fig. 6B). Importantly, these tumors also exhibited significant lamin A cleavage and downregulation of Bcl-2 and COX IV compared to the control tumors (Fig. 6B). These data are consistent with our in vitro data, and strongly indicate the potential of mortalin as a novel therapeutic target for MTC treatment.

Discussion

The present study reports that mortalin upregulation may facilitate MTC cell survival and proliferation by regulating multiple parallel independent cellular processes, including mitochondrial metabolism, MEK/ERK signaling, RET expression, and TP53 activity. Intriguingly, whereas transient MEK/ERK activation was necessary for mortalin depletion to induce cell cycle arrest, the pathway was not required for cell death induction. In contrast, mitochondrial damage was necessary for the cell death induction, but not for cell cycle arrest. However, although regulated, TP53 was not required for mortalin depletion to induce

cell death or growth arrest. These results suggest that mortalin may regulate a wide extent of physiological processes in cancer beyond its known role for TP53regulation, further expanding the role of mortalin in cancer.

Mitochondria are subcellular organelles that produce energy, building blocks, and signals for cell survival and death. These important functions of mitochondria are often dysregulated in cancer, providing a target for therapy [27]. Mortalin was mainly localized in mitochondria in MTC cells and its depletion was accompanied by profound depolarization of mitochondrial membrane, ROS generation, and apoptotic cell death in MTC cells. This observation indicates that mitochondrial damages are a major mechanism underlying MTC cell death upon mortalin depletion, suggesting the significance of mitochondrial function for MTC cell survival. Of note, we previously demonstrated that interfering with mitochondrial bioenergetics using the mitochondria-targeting small molecule compound, Mito-CP, could effectively suppress growth and survival of human MTC cell lines in culture as well as in mouse xenografts, which was accompanied by RET downregulation [30]. Therefore, our previous and current studies consistently suggest that mitochondrial targeting has potential as a therapeutic strategy to effectively induce MTC cell death, which would be a more desirable effect for cancer therapy. Mortalin may provide a specific target for development of this strategy.

MEK/ERK activation was necessary for mortalin depletion to induce growth arrest, although it was not required for cell death. We previously reported that MTC cells undergo cell cycle arrest in response to Raf/MEK/ERK activation without any notable sign of cell death, proposing that the pathway can function in a growth inhibitory context in MTC cells [22-26]. Our current observation of mortalin depletion effects on Raf/MEK/ERK signaling in MTC cells continuously supports this hypothesis. By extension, it may be conceivable that mortalin upregulation modulates Raf/MEK/ERK activity in MTC cells in the face of RET or Ras mutations so that tumor cells may bypass growth arrest responses, which are often associated with aberrant receptor tyrosine kinase or Ras activity [31]. It may also be conceivable that mortalin upregulation has a significant role in the reprogramming of mitochondrial metabolism and bioenergetics in MTC. Metabolic reprogramming is currently appreciated as an early event critical to tumorigenesis [32]. As such, mortalin may facilitate MTC cell proliferation and survival, and its overexpression may thus represent an important selection step for MTC cells to gain a growth/survival advantage.

Increasing evidence suggests that molecular chaperones can facilitate tumorigenesis by altering the stability or activity of important kinases and tumor suppressors [33]. Although mortalin largely shares the characteristics of HSP70 molecular chaperones [34, 35], it is possible that mortalin may have specific clients in different cancer types. It is therefore important to identify the effectors for mortalin function. Of note, it was reported that mortalin serves as a key regulatory protein for the import of mitochondrial ATPase components [36]. Whether this function has a relevance to aforementioned mortalin effects in MTC cells will have to be addressed in our future study. Likewise, it is also required to elucidate by what mechanism mortalin is upregulated in MTC. Since mortalin is inducible by nutritional stresses such as glucose deprivation [37], mortalin upregulation may be attributed to an increasing demand for nutrients during MTC development. Further

elucidation of the mechanisms underlying mortalin function and its upregulation in MTC may lead to an advanced therapeutic strategy for MTC.

In conclusion, our study characterizes mortalin as a key regulator of proliferation and survival of MTC cells, proposing mortalin as a novel target that may provide a distinct strategy for MTC therapy.

Materials and methods

Cell culture and reagents

TT and MZ-CRC-1 were maintained as previously described [30, 38]. TMRE, puromycin, G418, doxycycline, oligomycin, FCCP, and antimycin A were purchased from Sigma. Carboxy-H_2DCFDA, AZD6244, and Z-VAD(OMe)-FMK were purchased from Invitrogen, Selleck Chemicals (Houston, TX), and Millipore (Billerica, MA), respectively.

RNA interference

Construction of the pLL3.7 lentiviral mortalin-targeting shRNA constructs (shMort #1 and shMort #2) was previously described [12]. The pTRIPZ doxycyclineinducible microRNA-adapted shRNA targeting human mortalin was purchased from Open Biosystems (V3THS_362249). TP53 was depleted using two pLKO.1 lentiviral shRNA systems (Sigma-Aldrich, TRCN3754 and TRCN3756). MEK1 and MEK2 were depleted using lentiviral shRNA systems constructed in pLL3.7, which target GCAACUCAUGGUUCAUGCU in human MEK1 RNA (shMEK1) and GAAGGAGAGCCUCACAGCA in human MEK2 RNA (shMEK2).

Recombinant lentiviral constructs

pHAGE-HA-Mort* was generated by mutagenizing the full length human mortalin cDNA using the Quickchange II site-directed mutagenesis kit (Agilent Technologies, Santa Clara, CA) and the primers, ATATTGAAAATATGGTAAAGAACGCCGAGAAATATGCTGAAG and CTTCAGCATATTTCTCGGCGTTCTTTACCATATTTTCAATAT. pHAGE-Bcl-2 was previously described [12]. Lentivirus was produced as previously described [12].

Cell proliferation, death, and cell cycle assays

Cell viability was measured by counting trypan blue-stained cells using hemocytometer or by the colorimetric MTT assay, as previously described [39]. Annexin V (Invitrogen) was stained according to manufacturer's instruction. Cell cycle analysis was conducted using Hoechst 33342 as previously described [30].

Detection of mitochondrial membrane potential, oxidative stress, and extracellular flux

Cells were stained with TMRE or carboxy-H_2DCFDA, as previously described [30]. Oxygen consumption rates and extracellular acidification rates were determined using a XF96 Extracellular Flux Analyzer (Seahorse Bioscience), as previously described [40].

Immunoblot analysis

Immunobloting was conducted as previously described [12]. Antibodies were diluted as follows: mortalin/GRP75, 1:2500: ERK1/2, 1:2,500; phospho-ERK1/2 (Thr202/Tyr204), 1:2,500; GAPDH, 1:5,000; RET, 1:1,000 (sc-167, Santa Cruz Biotechnology, Santa Cruz, CA); PARP, 1:1,000; Bcl-2, 1:2,000; Bcl-xL, 1:2,000; COX IV, 1:2000 (Cell Signaling); phospho-RET (Tyr1062), 1:1,000 (R&D Systems). The Supersignal West Femto and Pico chemiluminescence kits (Pierce) were used for visualization of the signal. Images of immunoblots were taken and processed using ChemiDoc XRS+ and Image Lab 3.0 (Bio-Rad).

Immunofluorescence

Cells grown on chamber slides were washed with PBS, fixed with 3% paraformaldehyde, and incubated overnight at 4°C with the monoclonal antibody specific to mortalin (1:200, Santa Cruz Biotechnology, sc-133137) or the polyclonal antibody specific to COX IV (1:300, Cell Signaling, #4850). Cells were then double-stained with secondary anti- mouse Alexa Fluor 594 and anti-rabbit Alexa Fluor 488 (Invitrogen) conjugates at 1:200 dilution as described previously [41]. Images were acquired using a LCM510 microscope (Zeiss) and analyzed with proprietary AIM 4.2 software.

RT-PCR of RET, CT, and CGRP

RT-PCR was conducted using the reaction conditions and the primers previously described [30].

Immunohistochemistry

Formalin-fixed, paraffin-embedded 5 μm sections of three non-overlapping thyroid carcinoma tissue microarrays (TH801, TH802, and TH806), containing 38 MTC cases and 46 normal thyroid samples were purchased from US Biomax (Rockville, MD). All tissue samples consisted of uniform cores (1.5 mm in diameter, 2 cores per case for 32 carcinoma and 8 normal cases, 1 core per case for 6 carcinoma and 38 normal cases). The specimens were analyzed using monoclonal anti-mortalin antibody, D-9 (Santa Cruz Biotechnology, sc-133137), as previously described [12]. The specificity of this staining was validated with normal IgG type 2.

Tumor xenograft studies

1×10^7 cells in 200 μl Hank's balanced salt solution were inoculated subcutaneously into the rear flanks of 6-week-old female athymic nude (*nu/nu*) mice (Charles River Laboratories). Once palpable, tumors were measured using Vernier calipers at intervals indicated in the text. Tumor volumes were calculated using the formula: length x width x height x 0.5236. When tumor volumes reached 100 mm^3, mice bearing each cell line were sorted into two groups of 5 to achieve equal distribution of tumor size in all treatment groups. Treatment groups received 2 mg/ml of doxycycline (Sigma) in drinking water for 20 days, and control groups received pure water. After 10 days of administration, 2 animals from each group were euthanized by CO_2 asphyxiation. Tumor samples were collected and analyzed as previously described [30, 38]. Upon finishing the schedule for doxycycline treatment, animals

were observed for tumor relapse until tumor size reaches 2×10^3 mm^3. All animal studies were performed according to protocols approved by the Institutional Animal Care and Use Committee at Medical College of Wisconsin.

Statistical analysis

Unless otherwise specified, two-tailed unpaired student's t-test was used to assess the statistical significance of two data sets. The significance of immunohistochemistry data of human MTC tissues was determined by Mann-Whitney test. P values of < 0.05 were considered statistically significant.

Supplementary Material

Refer to Web version on PubMed Central for supplementary material.

Acknowledgements

We thank Dr. Sergey Tarima at the Division of Biostatistics, Medical College of Wisconsin (MCW) for statistical analysis; Dr. Alexandra F. Lerch-Gaggl (Pediatric BioBank & Analytical Tissue Core, MCW) for imaging immunohistochemistry data; and the MCW Cancer Center Bioenergetics shared resource and Advancing Healthier Wisconsin for Seahorse analysis. This work was supported by the American Cancer Society (RSGM-10-189-01-TBE) and the National Cancer Institute (R01CA138441) to J.I.P.

References

1. Tuttle RM, Ball DW, Byrd D, Daniels GH, Dilawari RA, Doherty GM, et al. Medullary carcinoma. J Natl Compr Canc Netw. 2010; 8:512–530. [PubMed: 20495082]
2. Agrawal N, Jiao Y, Sausen M, Leary R, Bettegowda C, Roberts NJ, et al. Exomic sequencing of medullary thyroid cancer reveals dominant and mutually exclusive oncogenic mutations in RET and RAS. J Clin Endocrinol Metab. 2013; 98:E364–369. [PubMed: 23264394]
3. Boichard A, Croux L, Al Ghuzlan A, Broutin S, Dupuy C, Leboulleux S, et al. Somatic RAS mutations occur in a large proportion of sporadic RET-negative medullary thyroid carcinomas and extend to a previously unidentified exon. J Clin Endocrinol Metab. 2012; 97:E2031–2035. [PubMed: 22865907]
4. Ciampi R, Mian C, Fugazzola L, Cosci B, Romei C, Barollo S, et al. Evidence of a Low Prevalence of RAS Mutations in a Large Medullary Thyroid Cancer Series. Thyroid. 2013; 1:1–8.
5. Degrauwe N, Sosa JA, Roman S, Deshpande HA. Vandetanib for the treatment of metastatic medullary thyroid cancer. Clin Med Insights Oncol. 2012; 6:243–252. [PubMed: 22723734]
6. Nagilla M, Brown RL, Cohen EE. Cabozantinib for the treatment of advanced medullary thyroid cancer. Adv Ther. 2012; 29:925–934. [PubMed: 23104465]
7. Wells SA Jr. Robinson BG, Gagel RF, Dralle H, Fagin JA, Santoro M, et al. Vandetanib in patients with locally advanced or metastatic medullary thyroid cancer: a randomized, double-blind phase III trial. J Clin Oncol. 2012; 30:134–141. [PubMed: 22025146]
8. Daugaard M, Rohde M, Jaattela M. The heat shock protein 70 family: Highly homologous proteins with overlapping and distinct functions. FEBS Lett. 2007; 581:3702–3710. [PubMed: 17544402]
9. Deocaris CC, Widodo N, Ishii T, Kaul SC, Wadhwa R. Functional significance of minor structural and expression changes in stress chaperone mortalin. Ann N Y Acad Sci. 2007; 1119:165–175. [PubMed: 18056964]
10. Kaul SC, Deocaris CC, Wadhwa R. Three faces of mortalin: a housekeeper, guardian and killer. Exp Gerontol. 2007; 42:263–274. [PubMed: 17188442]
11. Wadhwa R, Takano S, Kaur K, Deocaris CC, Pereira-Smith OM, Reddel RR, et al. Upregulation of mortalin/mthsp70/Grp75 contributes to human carcinogenesis. Int J Cancer. 2006; 118:2973–2980. [PubMed: 16425258]

12. Wu PK, Hong SK, Veeranki S, Karkhanis M, Starenki D, Plaza JA, et al. A Mortalin/HSPA9-Mediated Switch in Tumor-Suppressive Signaling of Raf/MEK/Extracellular Signal-Regulated Kinase. Mol Cell Biol. 2013; 33:4051–4067. [PubMed: 23959801]
13. Leustek T, Dalie B, Amir-Shapira D, Brot N, Weissbach H. A member of the Hsp70 family is localized in mitochondria and resembles Escherichia coli DnaK. Proc Natl Acad Sci U S A. 1989; 86:7805–7808. [PubMed: 2682628]
14. Dundas SR, Lawrie LC, Rooney PH, Murray GI. Mortalin is over-expressed by colorectal adenocarcinomas and correlates with poor survival. J Pathol. 2005; 205:74–81. [PubMed: 15532096]
15. Wadhwa R, Takano S, Robert M, Yoshida A, Nomura H, Reddel RR, et al. Inactivation of tumor suppressor p53 by mot-2, a hsp70 family member. J Biol Chem. 1998; 273:29586–29591. [PubMed: 9792667]
16. Lu WJ, Lee NP, Kaul SC, Lan F, Poon RT, Wadhwa R, et al. Mortalin-p53 interaction in cancer cells is stress dependent and constitutes a selective target for cancer therapy. Cell Death Differ. 2011; 18:1046–1056. [PubMed: 21233847]
17. Kaul SC, Aida S, Yaguchi T, Kaur K, Wadhwa R. Activation of wild type p53 function by its mortalin-binding, cytoplasmically localizing carboxyl terminus peptides. J Biol Chem. 2005; 280:39373–39379. [PubMed: 16176931]
18. Iosefson O, Azem A. Reconstitution of the mitochondrial Hsp70 (mortalin)-p53 interaction using purified proteins--identification of additional interacting regions. FEBS Lett. 2010; 584:1080–1084. [PubMed: 20153329]
19. Lu WJ, Lee NP, Kaul SC, Lan F, Poon RT, Wadhwa R, et al. Induction of mutant p53- dependent apoptosis in human hepatocellular carcinoma by targeting stress protein mortalin. Int J Cancer. 2011; 129:1806–1814. [PubMed: 21165951]
20. Wadhwa R, Yaguchi T, Hasan MK, Taira K, Kaul SC. Mortalin-MPD (mevalonate pyrophosphate decarboxylase) interactions and their role in control of cellular proliferation. Biochem Biophys Res Commun. 2003; 302:735–742. [PubMed: 12646231]
21. Ichihara M, Murakumo Y, Takahashi M. RET and neuroendocrine tumors. Cancer Lett. 2004; 204:197–211. [PubMed: 15013219]
22. Park JI, Strock CJ, Ball DW, Nelkin BD. The Ras/Raf/MEK/extracellular signal- regulated kinase pathway induces autocrine-paracrine growth inhibition via the leukemia inhibitory factor/JAK/STAT pathway. Mol Cell Biol. 2003; 23:543–554. [PubMed: 12509453]
23. Park JI, Strock CJ, Ball DW, Nelkin BD. Interleukin-1beta can mediate growth arrest and differentiation via the leukemia inhibitory factor/JAK/STAT pathway in medullary thyroid carcinoma cells. Cytokine. 2005; 29:125–134. [PubMed: 15613280]
24. Arthan D, Hong SK, Park JI. Leukemia inhibitory factor can mediate Ras/Raf/MEK/ERK-induced growth inhibitory signaling in medullary thyroid cancer cells. Cancer Lett. 2010; 297:31–41. [PubMed: 20570039]
25. Sosonkina N, Starenki D, Park JI. The Role of STAT3 in Thyroid Cancer. Cancers (Basel). 2014; 6:526–544. [PubMed: 24662939]
26. Park JI. Growth arrest signaling of the Raf/MEK/ERK pathway in cancer. Front Biol (Beijing). 2014; 9:95–103. [PubMed: 24999356]
27. Sarosiek KA, Ni Chonghaile T, Letai A. Mitochondria: gatekeepers of response to chemotherapy. Trends Cell Biol. 2013; 23:612–619. [PubMed: 24060597]
28. Weinberg F, Hamanaka R, Wheaton WW, Weinberg S, Joseph J, Lopez M, et al. Mitochondrial metabolism and ROS generation are essential for Kras-mediated tumorigenicity. Proc Natl Acad Sci U S A. 2010; 107:8788–8793. [PubMed: 20421486]
29. Ryter SW, Kim HP, Hoetzel A, Park JW, Nakahira K, Wang X, et al. Mechanisms of cell death in oxidative stress. Antioxid Redox Signal. 2007; 9:49–89. [PubMed: 17115887]
30. Starenki D, Park JI. Mitochondria-targeted nitroxide, Mito-CP, suppresses medullary thyroid carcinoma cell survival in vitro and in vivo. J Clin Endocrinol Metab. 2013; 98:1529–1540. [PubMed: 23509102]
31. Mooi WJ, Peeper DS. Oncogene-induced cell senescence--halting on the road to cancer. N Engl J Med. 2006; 355:1037–1046. [PubMed: 16957149]

32. Ward PS, Thompson CB. Metabolic reprogramming: a cancer hallmark even warburg did not anticipate. Cancer Cell. 2012; 21:297–308. [PubMed: 22439925]
33. Khalil AA, Kabapy NF, Deraz SF, Smith C. Heat shock proteins in oncology: Diagnostic biomarkers or therapeutic targets? Biochim Biophys Acta. 2011; 1816:89–104. [PubMed: 21605630]
34. Kampinga HH, Craig EA. The HSP70 chaperone machinery: J proteins as drivers of functional specificity. Nat Rev Mol Cell Biol. 2010; 11:579–592. [PubMed: 20651708]
35. Bukau B, Horwich AL. The Hsp70 and Hsp60 chaperone machines. Cell. 1998; 92:351–366. [PubMed: 9476895]
36. Schneider HC, Berthold J, Bauer MF, Dietmeier K, Guiard B, Brunner M, et al. Mitochondrial Hsp70/MIM44 complex facilitates protein import. Nature. 1994; 371:768–774. [PubMed: 7935837]
37. Merrick BA, Walker VR, He C, Patterson RM, Selkirk JK. Induction of novel Grp75 isoforms by 2-deoxyglucose in human and murine fibroblasts. Cancer Lett. 1997; 119:185–190. [PubMed: 9570370]
38. Starenki D, Singh NK, Jensen DR, Peterson FC, Park JI. Recombinant leukemia inhibitory factor suppresses human medullary thyroid carcinoma cell line xenografts in mice. Cancer Lett. 2013; 339:144–151. [PubMed: 23856028]
39. Hong SK, Yoon S, Moelling C, Arthan D, Park JI. Noncatalytic function of ERK1/2 can promote Raf/MEK/ERK-mediated growth arrest signaling. J Biol Chem. 2009; 284:33006–33018. [PubMed: 19805545]
40. Cheng G, Zielonka J, Dranka BP, McAllister D, Mackinnon AC Jr. Joseph J, et al. Mitochondria-targeted drugs synergize with 2-deoxyglucose to trigger breast cancer cell death. Cancer Res. 2012; 72:2634–2644. [PubMed: 22431711]
41. Sosonkina N, Nakashima M, Ohta T, Niikawa N, Starenki D. Down-regulation of ABCC11 protein (MRP8) in human breast cancer. Exp Oncol. 2011; 33:42–46. [PubMed: 21423094]

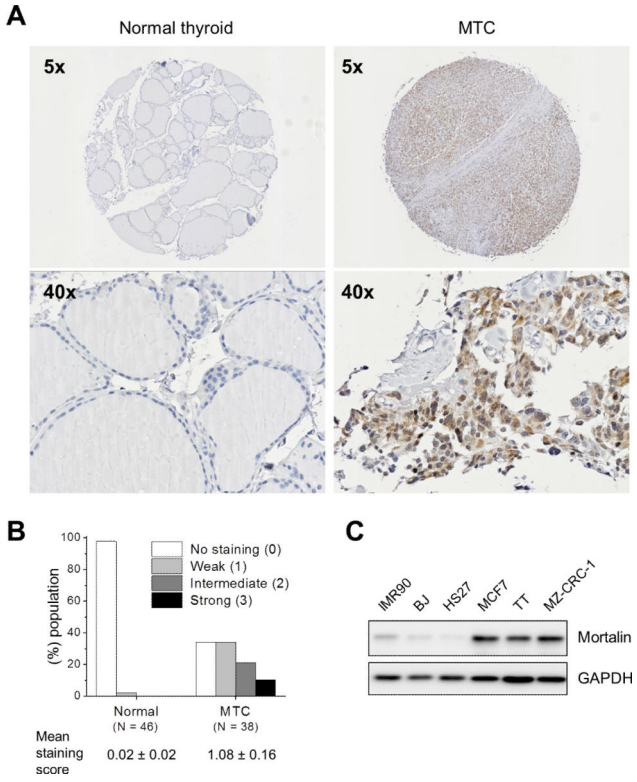

Figure 1. Mortalin is upregulated in human MTC

A and B, immunohistochemical analysis of mortalin protein in patient tissue biopsy specimens. **A,** representative IHC images, corresponding H&E staining shown in Supplemental Fig. S1. **B,** Mortalin expression in 46 normal thyroid and 38 MTC patient tumor tissues mortalin protein ($P < 0.0001$, Mann-Whitney test). **C,** Western blot analysis of mortalin expression in total cell lysates of the human MTC cell lines, TT and MZ-CRC-1. MCF7 and the primary normal fibroblasts were used as the positive and negative controls for mortalin expression, respectively. Glyceraldehyde-3-phosphate dehydrogenase (GAPDH) was used as a loading control.

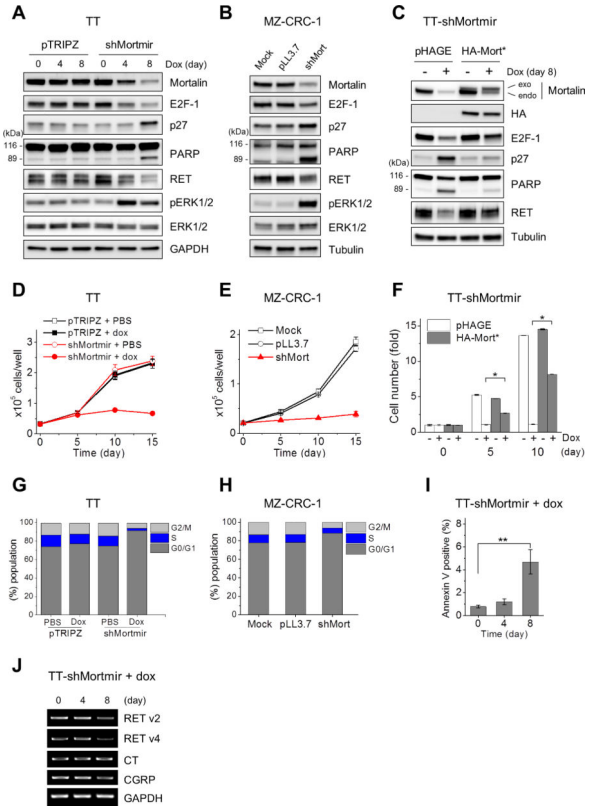

Figure 2. Mortalin knockdown induces growth inhibition in MTC lines

A and B, TT and MZ-CRC-1 cells were infected with doxycycline (dox)-inducible pTRIPZ and pLL3.7 viruses, respectively, which harbor shRNA constructs that target different sites on mortalin mRNA (shMortmir and shMort, respectively). Uninfected (mock)- or empty virus-infected cells were used for comparison. Data are representing images of multiple Western blot analyses of total lysates of TT treated with dox for indicated time and MZ-CRC-1 infected for 8 days. **C,** TT cells stably infected with pTRIPZ-shMortmir were infected with lentiviral pHAGE expressing N-terminal HA-tagged non-shMort-targetable mortalin mRNA (HA-Mort*). Western blot analysis of total cell lysates indicate that HA-Mort-shfree can abrogate mortalin knockdown effects. Empty pHAGE was used as the control. **D and E,** Proliferation rates of cells in A and B were monitored by cell counting Data (mean ±SD, n=4), *P < 0.0001. **F,** Viability of cells in C was monitored by 3-(4,5-dimethyl-2-thiazolyl)-2,5-diphenyltetrazolium bromide (MTT) assay at indicated time points. Data (mean ±SD, n=4) are expressed as fold changes relative to the value of initial cell culture. *P < 0.001. **G and H,** Cell cycle was determined in cells in A and B using Hoechst 33342 at the treatment day 8. **I,** Annexin V staining of TT cells in A. Data (mean ± SD) are from an experiment in triplicate. **J,** RT-PCR analysis of RET and the calcitonin splicing variants, CT and CGRP using total RNA of TT cells in A. GAPDH was the control for equal amounts of RNA used.

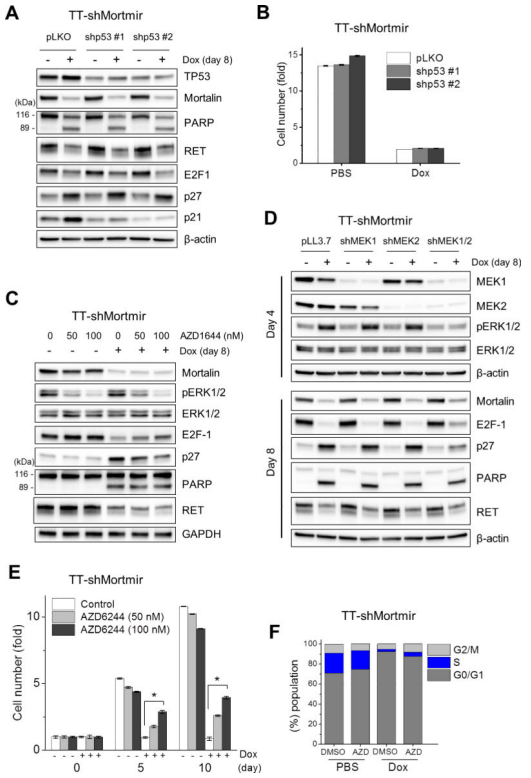

Figure 3. TP53 and MEK/ERK mediates differential effects of mortalin depletion in TT cells

A and B, TT-shMortmir cells were infected with lentiviral pLKO.1 expressing two different TP53-targeting shRNAs (shp53#1 and shp53#2) during dox treatment. Empty pLKO.1 is the controls for shp53. A, Western blot analysis of total cell lysates. B, Cell viability was monitored by MTT assay at dox treatment day 8. Data (mean ±SD, n=4) are expressed as fold changes relative to the value of initial cell culture. **C,** Western blot analysis of total lysates of TT-shMortmir cells treated with AZD6244 during dox treatment. Equal volume of DMSO was used as the control for AZD6244. **D,** Western blot analysis of total lysates of TT-shMortmir cells infected, either singly or doubly, with lentiviral pLL3.7 expressing shRNA targeting MEK1 and MEK2 (shMEK1 and shMEK2, respectively) during dox treatment. **E,** Cell viability was monitored by MTT assay at dox treatment day 8. Data (mean ±SD, n=4) are expressed as fold changes relative to the value of initial cell culture. *P < 0.001. **F,** Cell cycle analysis of cells in C.

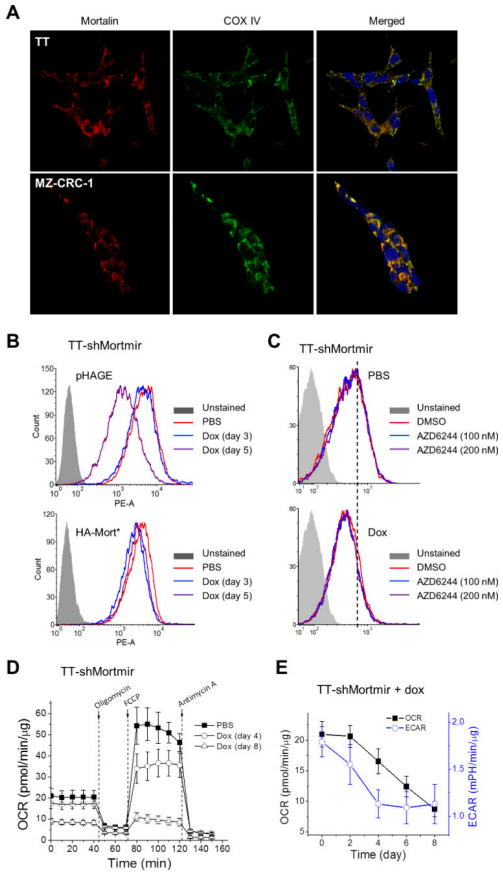

Figure 4. Mortalin depletion induces loss of mitochondrial membrane potential, decreased oxygen consumption, and increased acidification in MTC cells

A, Immunofluoresence analysis of mortalin localization in TT and MZ-CRC-1 cells. COX IV serves as a marker specific to mitochondria. Areas of overlap are seen as yellow. **B,** TT-shMortmir cells, infected with empty pHAGE (top panel) or pHAGE expressing HA-Mort-shfree (bottom panel), were treated with doxycycline for indicated time prior to TMRE staining. Changes in the mitochondrial membrane potential were determined by flow cytometry measurement of red fluorescence (PE channel, 575 nm). **C,** In the presence of AZD6244, TT-shMortmir cells were treated with PBS (top panel) or dox (bottom panel) for 4 days prior to TMRE staining. **D,** Determination of OCR in TT-shMortmir cells treated with dox for indicated time. Five baseline OCR measurement were taken before injecting oligomycin (1 μg/ml), FCCP (2 μmol/l), and antimycin A (10 μmol/l). Data are mean ± SD, n=6. **E,** Determination of baseline OCR and ECAR in TT-shMortmir cells treated with dox for indicated time. Data (mean ± SD, n=6) were normalized to protein amounts.

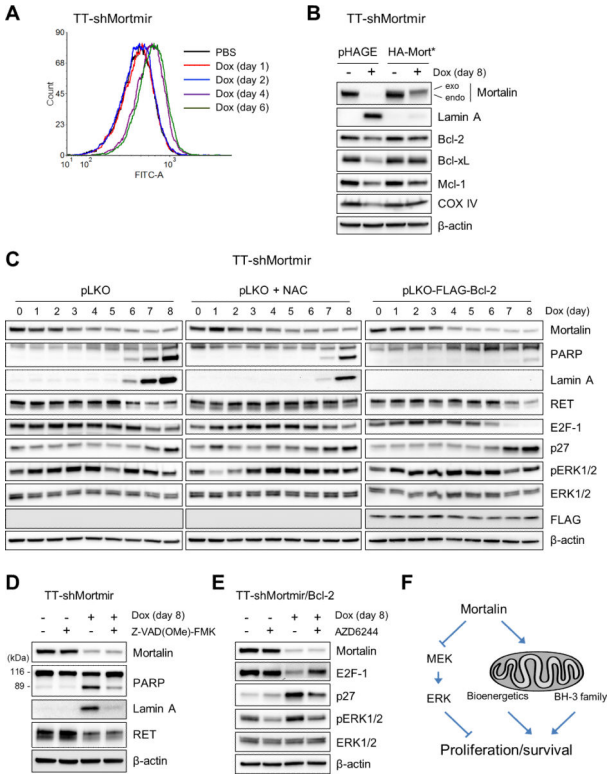

Figure 5. Mortalin depletion induces oxidative stress and Bcl-2 family-dependent cell death

A, To determine ROS generation, fluorescence of carboxy-H_2DCFDA in TT-shMortmir cells treated with dox for indicated time was measured by flow cytometry (FITC channel, 525 nm). **B,** Western blot analysis of TT-shMortmir cells infected with lentiviral pHAGE expressing HA-Mort* during dox treatment. Empty pHAGE is the control. **C,** Western blot analysis of TT-shMortmir cells treated with the ROS scavenger NAC (5 mM) or infected with lentiviral pLKO expressing Bcl-2. Empty pLKO is the control. **D,** Western blot analysis of TT-shMortmir cells treated with the pan-caspase inhibitor, Z-VAD(OMe)-FMK (20 μM) during dox treatment. PARP and Lamin A are substrates of caspase 3 and 6, respectively. **E,** Western blot analysis of Bcl-2-overexpressing TT-shMortmir cells treated with 100 nM AZD6244. Total cell lysates were used for Western blotting in B to E. **F,** Proposed model. Mortalin affects proliferation and survival of MTC cells by regulating the MEK/ERK pathway and mitochondrial metabolism in MTC cells. The mechanisms by which mortalin regulates MEK/ERK activity and mitochondrial bioenergetics is yet to be determined. See the text for details.

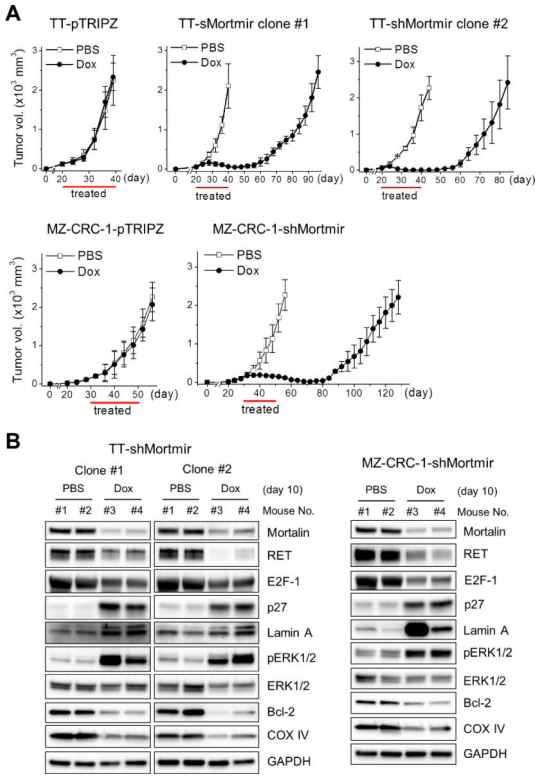

Figure 6. Mortalin depletion suppresses MTC xenografts in mice

A, Clones of TT-shMortmir and MZ-CRC-1-shMortmir, and their control pTRIPZ clones were xenografted into athymic mice. Dox (2 mg/ml) was administered via drinking water and tumor sizes were measured according to the schedule shown in the graphs. Data are mean ± SEM (n=3). **B,** Western blot analysis of tumor homogenates harvested from two mice in each group in A at dox administration day 10.